Egyptian Journal of Petroleum (2016) **25**, 201–214

HOSTED BY

Egyptian Petroleum Research Institute

Egyptian Journal of Petroleum

www.elsevier.com/locate/egyjp
www.sciencedirect.com

FULL LENGTH ARTICLE

Structure roles for the localization of metasomatite uranium deposit type at Wadi Belih area, Northern Eastern Desert, Egypt

Anton G. Waheeb *, **Hassan I. El Sundoly**

Nuclear Materials Authority, Cairo, Egypt

Received 12 February 2015; accepted 6 May 2015
Available online 30 April 2016

KEYWORDS

Structure;
Uranium;
Stress analysis;
Radioactivity;
Metasomatite uranium type

Abstract Wadi (W.) Belih area is one of the most important uranium occurrences in the northern parts of Eastern Desert of Egypt. The major mineralizations are structurally controlled especially along the contact between the Hammamat sedimentary rocks and younger granites record a complex history of deformations where, the uranium mineralization are located along a footwall of shear zone striking ENE–WSW to NE–SW direction. This shear zone was reactivated during its tectonic history starting from compression trending NW–SE and NE–SW respectively to younger extensional event trending NW–SE.

Due to the resulting younger extension NW–SE event the hydrothermal solution gradually migrates upward forming alkali metasomatite, contemporaneous with uranium mineralization. They are developed along that shear zone where structure contact and the low-stress regions in the vicinity of the shear zone are favorable locations for fluid flow focusing and hence U mineralizations occur in the highly fractured and mylonitized zones along the contact as lensoidal bodies.
© 2015 The Authors. Production and hosting by Elsevier B.V. on behalf of Egyptian Petroleum Research Institute. This is an open access article under the CC BY-NC-ND license (http://creativecommons.org/licenses/by-nc-nd/4.0/).

1. Introduction

Based on the geological setting of the deposit (IAEA) classification, uranium deposits world-wide are grouped into 14 major categories of deposit types (Fig. 1). The authors suggests that W. Belih uranium mineralizations along the contact between Hammamat sediments and granites could be fitted within the metasomatite uranium deposit categories; where metasomatite uranium deposits occur in association with structurally-deformed rocks that were already altered by metasomatic processes, usually associated with the introduction of sodium into these rocks [1,2]. Uranium mineralization is contemporaneous with the metasomatism of the host rocks and the mineralization is structurally controlled with faults providing a focused pathway for fluid migration with mineralization concentrated along and adjacent to faults [4]. All the above mentioned criteria of the metasomatite uranium deposit type are detected in W. Belih area. Major examples of this type include Espinharas deposit (Brazil) and the Zheltye Vody deposit (Ukraine) and other similar types of U deposits are

* Corresponding author.
Peer review under responsibility of Egyptian Petroleum Research Institute.

http://dx.doi.org/10.1016/j.ejpe.2015.05.017
1110-0621 © 2015 The Authors. Production and hosting by Elsevier B.V. on behalf of Egyptian Petroleum Research Institute.
This is an open access article under the CC BY-NC-ND license (http://creativecommons.org/licenses/by-nc-nd/4.0/).

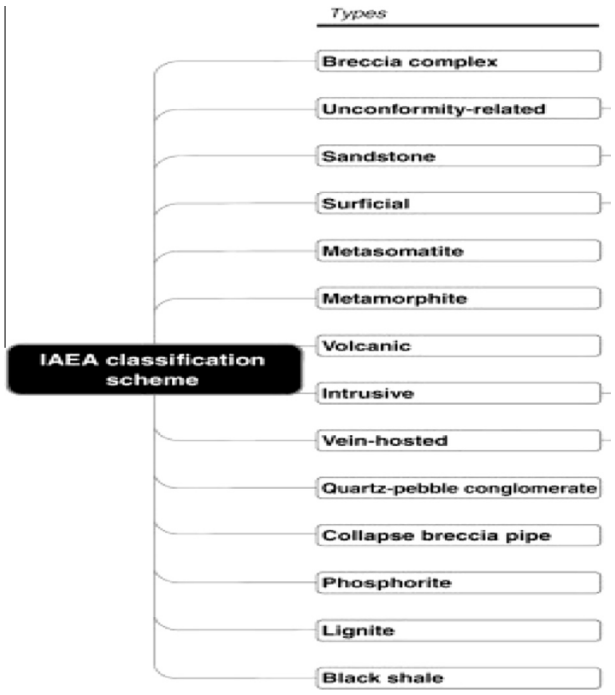

Figure 1 IAEA classification scheme of uranium ore deposits (after [3]).

known all over the world (Fig. 2). In the present work, W. Belih area near Gabal (G.) Gattar could be the Egyptian example.

The mineralizations are best hosted in the Hammamat sediments along the structure contact with sheared Gattar granites. Some mineralizations may, however, occur in the sheared granites itself [6–9,10].

The uranium mineralizations at the contact zone between G. Gattar and the Hammamat sedimentary rocks along W. Belih was investigated by [11]. He concluded that the uranium mineralization is essentially controlled by a local reverse fault trending ENE–WSW and dips 45–65° to the SSE.

X-ray diffraction technique was used by [12,13] to identify some secondary uranium minerals for the uranium mineralizations at part of the studied area and they mentioned the presence of uranophane and tyuyamunite as secondary uranium minerals.

Both granites and Hammamat sediments, at W. Belih, are enriched in U, Y, W, Nb, Cu, Pb, Sb and Zn elements, but with higher magnitude for the Hammamat [14].

The supergene meteoric water and super-heated solutions could pass through the structural network. They leached some of the magmatic U from the younger granites and reprecipitated their loads, in the shear and weak zones of the Hammamat sediments, by the effect of evaporation and adsorption on the surface of Fe oxides and clay minerals [15].

Detailed subsurface studies of the mineralized faults and fractures were carried out in mine located in the investigated area. These studies revealed that the presence of a major subsurface uranium mineralized trends recorded in the main adit and the drift of that mine. It takes essentially the ENE–WSW and NE–SW trends [16].

There is about twenty three uranium occurrences in G. Gattar granites, most of them are located near the granites – Hammamat sediments contact and very few are hosted in the Hammamat sediments [17].

In this paper, structural analysis along the uranium mineralized shear zone in the structural contact between Hammamat and granites are used to constrain the timing of deformation and fluid circulations to clarify the relationship between tectonic activity and uranium mineralizations.

2. Field geology

The investigated area is bounded by Latitudes 27°6′ and 27°7′ N and Longitudes 33°15′ and 33°18′ E (Fig. 3). The nearest

Figure 2 World distribution of uranium deposits associated with Na-metasomatism. The dark gray zones correspond to Archean to Early Paleoproterozoic rocks (after [5]).

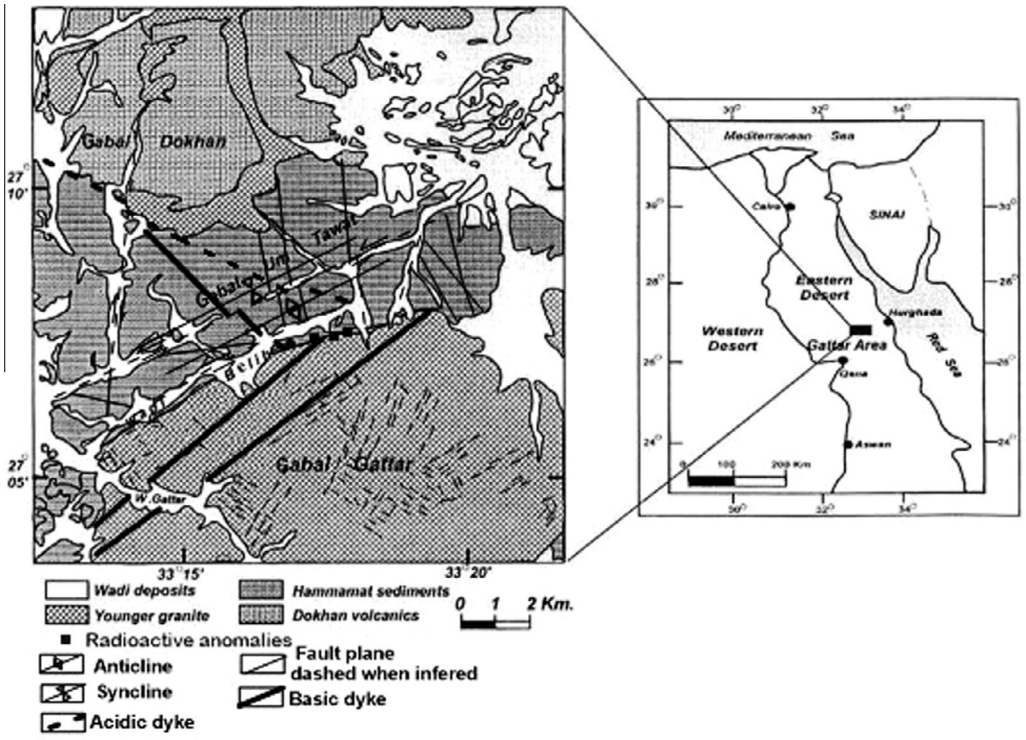

Figure 3 Geological and location map of W. Belih area, Northern Eastern Desert, Egypt (modified after [14]).

town is Hurghada; which lies on the Red Sea Coast. The main rock types exposed in the investigated area are Dokhan volcanics, Hammamat sedimentary rocks, younger granites, dykes and veins (Fig. 3).

In W. Belih area, the Hammamat sedimentary rocks are well exposed at G. Um Tawat, forming a relatively low hilly country between G. Dokhan volcanics and G. Gattar granites (Fig. 3). These sediments can be easily distinguished from the country rocks by their distinct bedding chronologically (Fig. 4).

The succession of the Hammamat sedimentary rocks, in the investigated area, consists of relatively coarse conglomeratic beds at the base, with fine graywacke and siltstone beds upward. Along the contact with G. Gattar granites, the Hammamat sedimentary rocks consist mainly of graywackes and siltstones. They range in color from light gray, dark gray to black, depending on their composition and alteration effects. They are highly foliated and laminated (Fig. 5).

The Hammamat sediments are extruded by the younger granites of G. Gattar with structural contact. In some places along this contact; the granites send offshoots into the Hammamat successions (Fig. 6).

The younger granite, in the study area, is outcropped south W. Belli forming moderately high rugged mountains. The

Figure 4 General view for subhorizontal beds of Hammamat sedimentary rocks, W. Belih area, looking NE.

Figure 5 General view for highly foliated Hammamat sedimentary rocks, W. Belih area, looking NW.

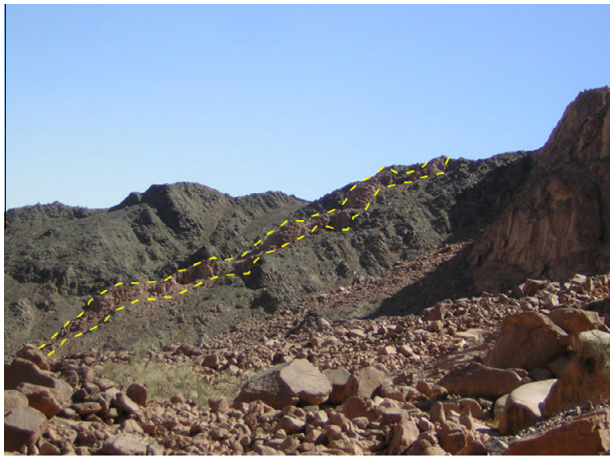

Figure 6 Offshoot of younger granites intruded into Hammamat successions, W. Belih area, looking E.

Figure 7 General view for moderately high rugged mountains of G. Gattar younger granites, W. Belih area, looking SE.

granitic rocks are coarse to medium grained and with a light pink to reddish pink color (Fig. 7).

The previously mentioned rocks are intruded by many dyke swarms of variable composition, dimensions and directions. These dykes are mainly represented by acidic, intermediate and basic ones (Fig. 8). These dykes are emplaced through weak and tensional structural planes predominating in the NE–SW to NNE–SSW trend with dip varying from 40° to 70° to the SE directions. These dykes have a unique relation with the younger granites where G. Gattar granites are only cut by basic dykes which are assigned as post granitic dykes. On the other hand, at the contact between granites and the Hammamat sedimentary rocks, the granites intrude the country rocks and their associated acidic and intermediate dykes and the intermediate dykes are never observed in the younger granite; so that, it is assigned as post Hammamat sedimentary rocks pre-younger granite. Some quartz veins and veinlets in association with pegmatite pockets and dykes are also observed.

Alkali metasomatic processes are very distinct, in many parts, along the contact between the Hammamat and the

Figure 8 Acidic dyke extruded into Hammamat sedimentary rocks, W. Belih area, looking NW.

granites. These processes have affected both the granites and the adjacent Hammamat sediments. The main products of these processes are several bodies of episyenitized granites (Fig. 9). The term episyenite characterizes a dequartzified granitic rock, the hydrothermal leaching of quartz from granites is associated with Na and/or K metasomatism [18]. The chemical composition of altered granites at the study area as well as the mass balance calculations suggest two distinct types of alteration, namely; Na- and K-metasomatism [19].

The marginal episyenitized granitic rocks are occasionally hosting uranium mineralizations. In addition, hematitization, silicification, kaolinitization, fluoritization, epidotization besides the frequent presence of manganese dendrites are the most pronounced wall rock alteration features due to these processes. The alteration features associated with the Hammamat sediments are the strong hematitization, which is usually in intimate association with the secondary uranium mineralizations, kaolinitization, epidotization, fluoritization, chloritization and manganese dendrites and bleaching (chemical reduction of iron) of some parts of the Hammamat sediments changing their original color from green to yellowish white.

Figure 9 Episyenitized granites due to alkali metasomatic processes along the contact between younger granite and Hammamat sedimentary rocks, W. Belih area, looking SE.

We must note that the direction of marginal episyenite granite is ENE–WSW to NE–SW direction parallel to the structural contact between the granite and Hammamat sedimentary rocks in addition to that the alkali metasomatic processes in association with uranium localization are very distinct also in the peripheral area between the granite and the Hammamat sedimentary rocks along the contact, this indicates that, the hot fluids use the ENE–WSW and NE–SW contact faults as pathway to flow up along it and cause this complicated series of metasomatic reactions and uranium deposition and localization.

3. Structure

The structural deformations, in the study area, are preserved in two strain states as a result of the stresses causing the deformation namely; ductile deformation (foliation and folds) and Brittle deformation (faults and joints). In the following paragraphs, these structures are described and geometrically analyzed.

3.1. Ductile deformation structures

The different rocks behave differently under stress; some rocks when subjected to stress are fractured or faulted, while others are folded and foliated during deformation and/or dynamic metamorphism. In W. Belih area, folding and foliation are the most remarkable ductile deformational fabrics clearly noticed in the Hammamat sedimentary rocks.

3.1.1. Folds

Folds are the most important structural elements that played an impressive role in the deformational history of the study area. Folds are clearly recognized in the Hammamat sedimentary rocks. At the contact with the younger granite a tight isoclinal recumbent fold with horizontal axis plunging 2° to N43° W is recorded (Fig. 10) and asymmetrical upright open anticline with truncated hinge of NE–SW fold with limbs dipping to SE and SW at moderate angels are observed near the contact along W. Belih (Fig. 11).

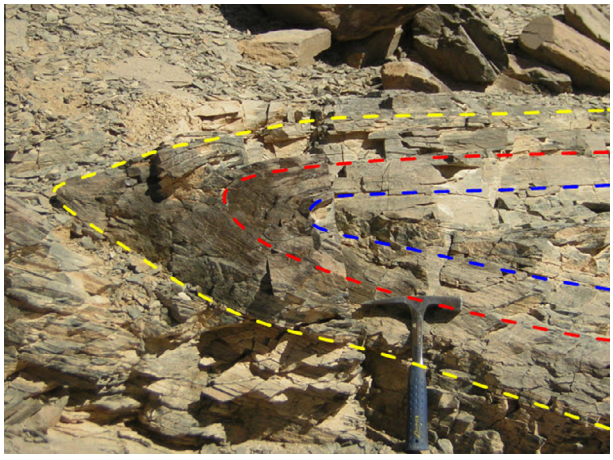

Figure 10 Tight isoclinal recumbent fold of NW–SE fold set in Hammamat sedimentary rocks at W. Belih area, looking N.

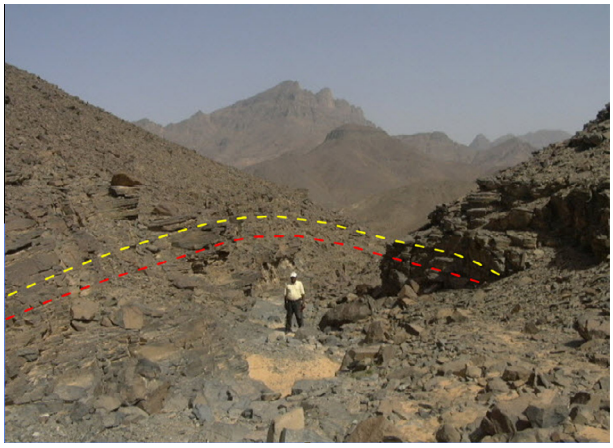

Figure 11 Asymmetrical upright open anticline with truncated hinge of NE–SW fold set at W. Belih area, looking NE.

The attitudes of 105 bedding planes were measured away from contact to north in the field and a Pi (π) diagram (Fig. 12) was constructed for their poles. The stereographic plots of the bedding planes, Pi (π) diagram; indicates an open major asymmetric anticlinal fold with NE–SW axis parallel to the main Wadi (W. Belih) in G. Um Tawat. As deduced from the Pi (π) diagram the fold axis is striking N38°E and plunging 5° to SW (Fig. 12).

Accordingly, the bedding of Hammamat sedimentary rocks represents a broad open anticlinal fold with a fold axis striking NE–SW and gently plunging to SW reflecting NW–SE compressional trend in a direction perpendicular to the direction of fold axis (Fig. 12).

3.1.2. Foliation

The attitudes of 100 foliation planes (Fig. 5) were measured in the field and stereographic projection was constructed for their

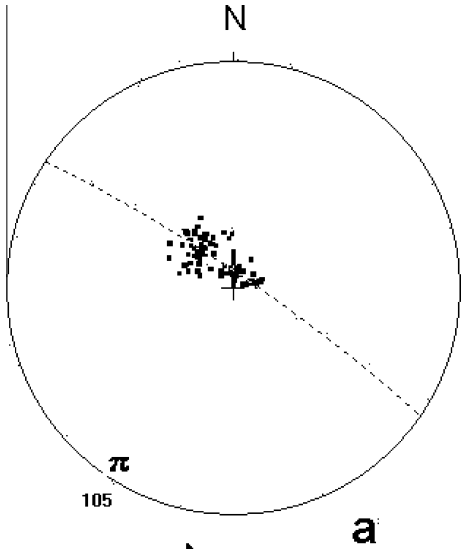

Figure 12 Pi (π) diagram of the geometrical analysis of 105 bedding planes of the Hammamat sedimentary rocks (dashed lines, great circle; small black circles, poles to bedding planes; π, fold axis).

poles and the distribution of their strikes (Fig. 13). The stereographic projection indicates that, the sets of foliations in the Hammamat sedimentary rocks are oriented in NE–SW as a general trend, revealing a compressional trend around the NW–SE direction (Fig. 13).

3.2. Brittle deformation structures

Faults and joints are the products of the brittle deformation affecting the various rock types of the study area. Rocks that yield by rupture when they are under a stress state split along definite planes.

3.2.1. Faults

W. Belih area is highly affected by different trends of faults with various types of sense of movements. They are normal and reverse dip slip faults, strike slip sinistral and dextral faults. Most of the faults are recognized in the field by separation of rock types and associated criteria, such as slickenside and intense shearing along fault zones (Figs. 14 and 15). The following is a description of the faults affecting the uranium mineralized area along the contact between the Hammamat sedimentary rocks and younger Gattarian granites.

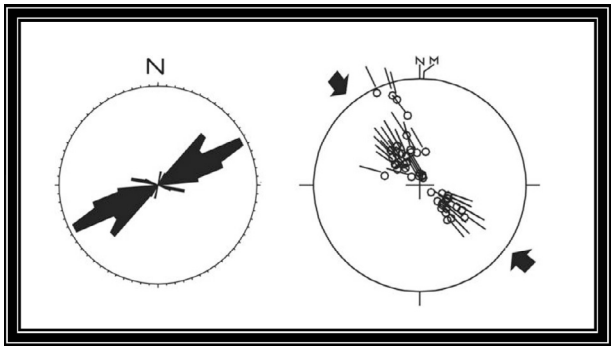

Figure 13 Rose diagram of 100 foliation planes strike and lower hemisphere stereographic projection showing the main stress trend.

Figure 14 Separation of pegmatitic dyke by NNW–SSE sinistral fault as indication for minor faulting, W. Belih area, top view.

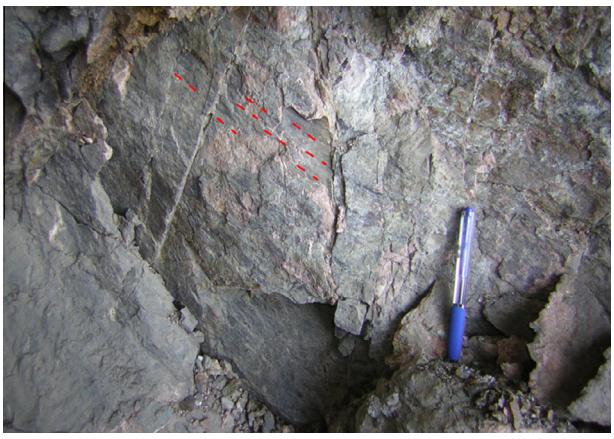

Figure 15 Slickenside and ribs observed at dextral NW–SE fault plane in the Hammamat sedimentary rocks, W. Belih area, looking SW.

Fault slip data analysis is carried out to reconstruct the paleostress axes through the calculation of reliable stress tensor represented by its components $\sigma1$, $\sigma2$ and $\sigma3$ and the ratio of the principal stress differences Φ ($\Phi = (\sigma2 - \sigma3)/(\sigma1 - \sigma3)$ [20], using the pressure/tension axes method (P/T method); this method calculates the theoretical compression (P) and tension (T) axes for each fault plane with lineations and known sense of movement [21] using computer program Win Tensor [22].

Fault slip data analysis was carried out at 11 locations along the contact between the Hammamat sedimentary rocks and younger granite. Field measurements of about 140 fault slip data revealed that, the contact zone is subjected to a compression regimes at first from NW–SE and then from NE–SW and finally to extensional regime from NW–SE (Table 1). The following is the description of the detailed analyses and computed tensors (Appendix 1).

3.2.2. Compressional events

Two compressional phases are defined in the Hammamat sedimentary rocks along the contact with younger granite and presented in Table 1. Compressional paleostress tensors are well determined in 7 stations. All of them are detected from strike-slip fault systems except one from reverse fault system. The strike-slip conjugate fault systems allowed the computation of 11 paleostress tensors in stations 1, 2, 3, 4, 6, 7 and 9 (Figs. 16 and 17). The calculated tensors of these phases define two main events: the NW–SE and NE–SW compressional trends.

The NW–SE major compressional event is computed from strike-slip fault systems at stations 2, 4, 6 and 7 and also from only one reverse fault at station 9 (Fig. 16). The computed $\sigma1$ for the NW–SE compressional trend plunges between 8° and 21° in directions around 126° and 129° and in a direction of 325° with plunge 24°. Most of the fault planes have very steeply to nearly vertical dip angles.

This event induced the major folding in the Hammamat sedimentary rocks around NE–SW horizontal axis (Fig. 12) at the contact with the younger granites and it also induced the NNW–SSE trending sinistral faults and NW–SE trending dextral faults and the ENE–WSW reverse fault. It is assigned to be the oldest one in W. Belih area, where all the field obser-

Table 1 Summary of successive tectonic phases detected in Hammamat sedimentary rocks along the contact with younger Gattarian granite.

Tectonic phase	Events	(σ1 or σ3)		Reactivated fault trends	Reference station
		Trend	Plunge		
NW–SE	EXT	130–143° and 306°	1–3°		5–8–12–14
NE–SW	CP	49° and 215–232°	29–38° and 14°	NE–SW ENE–WSW	1–2–3–4–7–9
NW–SE	CP	325° and 126–129°	24° and 8–21°	ENE–WSW	2–4–6–7–9

EXT = extension; CP = compression; σ1, for compression; σ3, for extension.

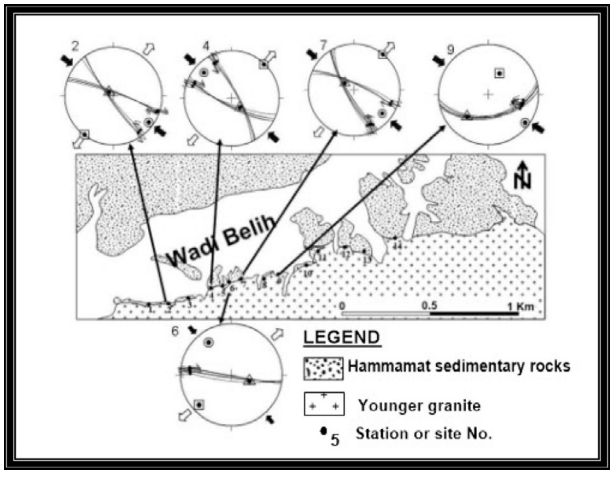

Figure 16 Analysis of thrust and strike slip fault plane data and compression paleostress tensors corresponding to NW–SE trend, W. Belih area.

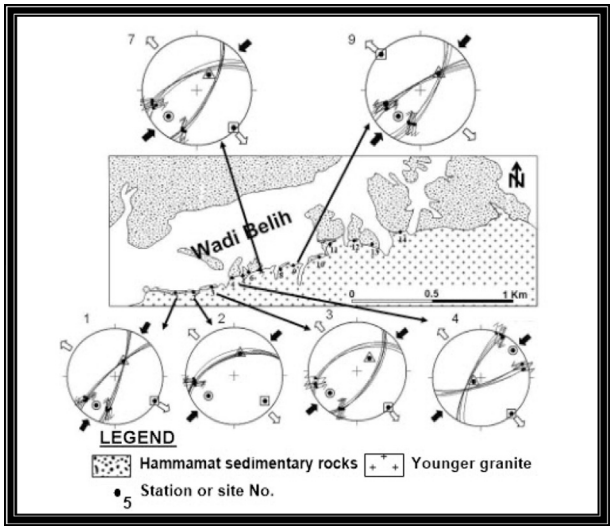

Figure 17 Analysis of strike slip fault plane data and compression paleostress tensors corresponding to NE–SW trend, W. Belih area.

vation indicates that; the NE–SW compressional event is computed from 5 conjugate strike-slip fault systems at stations 1, 3, 4, 7 and 9 and from the sinistral strike slip fault at station 2 (Fig. 17). The directions of σ1 range between 215° and 232° with plunges ranging between 29° and 38° and in a direction of 49° with plunge 14°. Most fault planes have high angles of dip. This event induced the mesoscopic folding in the Hammamat sedimentary rocks around the horizontal NW–SE fold axis (Fig. 10) at the contact with the younger granites and it also induced the NE–SW dextral faults and ENE–WSW sinistral faults. This compressional event reactivated moderately angel reverse fault that trends ENE–WSW as strike slip fault (station 9) belonging to the NW–SE compressional phase so that, this event is assigned to be younger than the NW–SE compression.

3.2.3. *Extensional events*

Only one extensional event is defined in the Hammamat sedimentary rocks along the contact with younger granite which is NW–SE extensional event and presented in Table 1.

The NW–SE extensional trend was computed from normal fault systems at only four stations (Fig. 18, stations 5, 8, 12 and 14). The directions of σ3 computed for this phase range between 130° and 143° and also 306° with plunges ranging between 1° and 3°. The strike of the fault planes is NE–SW and N–S. The geometrical relationships between the attitude of the fault planes and the slip direction (Fig. 18) indicated that this extensional event is a rejuvenated one to an older NW–SE extension event and this improved from the following field criteria there is NE–SW acidic and intermediate dykes invade the Hammamat sedimentary rocks but not the younger granite, in addition to that field observations indicate that NE–SW intermediate dykes are never observed in the younger granite but there is NE–SW to NNE–SSW trending basic dykes and pegmatitic pockets, related to this event, are recorded extruded across the footwall of the contact shear zone and parallel to

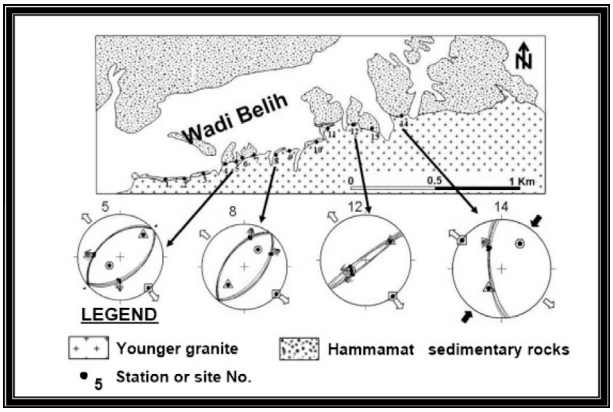

Figure 18 Analysis of the normal fault plane data and tension paleostress tensors corresponding to NW–SE trend, W. Belih area.

contact. This reveals that the NW–SE extension is initiated post Hammamat sedimentary rock pre-younger granite and rejuvenated again as post-younger granite event. It reactivated NE–SW and ENE–WEW strike slip faults belonging to the NE–SW compressional phase (Fig. 17, site 1 and 9); so that, this event is assigned as post NE–SW compressional event.

The investigated area is subjected to several deformation phases, the resultant general chronological sequence of detected events along the contact between the Hammamat sedimentary rocks and younger granite is arranged as the following using the previously described direct and indirect criteria.

During post Hammamat sedimentary rocks pre-younger granite time span the area was affected by NW–SE extensional phase. This phase induced the NE–SW normal faults before the emplacement of the younger granite, where field observations indicate that, the NE–SW acidic and intermediate dykes invade the Hammamat sedimentary rocks but never recorded in the younger granite. This indicates that, the NW–SE extension is initiated post-Hammamat and pre-younger granite.

The emplacement of the younger granite induced the local meso-folds in the bedding planes of the Hammamat sedimentary rocks at their contact, followed by the following tectonic events. The NW–SW compression event induced the NNW–SSE trending sinistral faults and NW–SE trending dextral faults and the ENE–WSW reverse faults. This event induced also the major folding of the Hammamat sedimentary bedding planes around the horizontal NE–SE fold axis.

The NE–SW compression represents the second event in the chronology along the contact area, which induced the NE–SW dextral faults and ENE – WSW sinistral faults. This event induced also the mesoscopic folding in the Hammamat sedimentary rocks around the horizontal NW–SE fold axis.

Finally the NW–SE extension event comes in the chronology along the contact between the Hammamat sedimentary rocks and younger granites which rejuvenate the NE–SW trending normal faults for the post Hammamat sedimentary rocks pre-younger granite intrusion and NE–SW and ENE–WSW strike slip faults belonging to NE–SW compression event accompanied with injection of basic post granitic dykes.

3.2.4. Joints

Joints recorded in W. Belih area are developed in a pronounced straight form and possess long extensions. The majority of joints are of tectonic origin and most of them are of shear type which are barren of any filers mainly parallel or sub-parallel to the major fault lines (Fig. 19). The tension type is also common and the most important tension joint filers, recorded in the study area, are uranium in addition to iron oxides, manganese oxides, quartz and epidote (Fig. 20). The tension joints affecting the rock types adjacent to the contact are structurally analyzed as follows.

A stereographic projection for 35 poles of tension joints is constructed and analyzed for stress analysis using improved right dihedron method [22] and determination of the three principle stress axes (Fig. 21). The following are the attitude of the three stress axes.

1. The principle stress axis $\sigma 1$ is plunging 33° on bearing 223°.
2. The intermediate stress axis $\sigma 2$ is plunging 48° on bearing 85°.
3. The least stress axis $\sigma 3$ is plunging 21° on bearing 329°.

Figure 19 Two conjugate shear joints in Hammamat sedimentary rocks, W. Belih area, and top view.

Figure 20 Tension joint filled with epidote in the Hammamat sedimentary rocks, W. Belih area, looking SW.

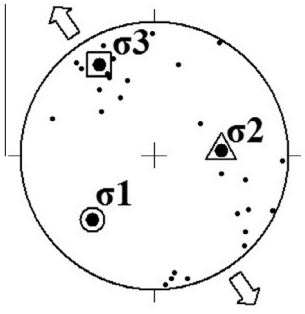

Figure 21 Diagram for an equal area stereographic projection of poles of 35 tension joints in W. Belih area adjacent to contact and the three principle stress axes for these joints.

The analysis of the different stress axes of tension joints in W. Belih area (Fig. 21) indicates that the area is subjected to extension force from NW–SE.

4. Radioactivity

The radiometric investigations was achieved using the gamma ray scintillometer; model RS-230 through field measurements, radiometric analytical measurements in terms of eU, eTh (ppm) and K (%) contents from collected samples for fresh Hammamat and mineralized Hammamat (Fig. 22 and Table 2). X-ray diffraction Technique (XRD) model Philips PW3710/31 at the Nuclear Materials Authority (NMA) to identify the minerals and the Environmental Scanning Electron Microscope ESEM-EDAX, at NMA and Military Lab were used to analyze the uranium minerals and investigate the morphological characteristics of the minerals as well as to give a semi quantitative evaluation of their elemental composition.

A systematic radiometric survey was carried out along the contact between the Hammamat and granites. A particular attention was paid to all structural features such as faults, shear zones and other alteration features as well as hydrothermal altered zones. Many radioactive anomalies were previously recorded; the authors studied the structural control and features for these anomalies. The most important anomalies will be described in the following paragraphs:

The first anomaly is represented by a lenticular zone of 15 × 5 m in dimensions (sample 7, Fig. 22). It is found along a major fault trending ENE–WSW to NE–SW (Fig. 23) with dips of about 73° to SE. This fault is a reactivated fault; it was in the beginning a thrust fault during the NW–SE compression regime then reactivated as sinistral fault during

Figure 23 Radioactive NE–SW oblique fault plane with visible secondary uranium mineral, W. Belih area, looking SW.

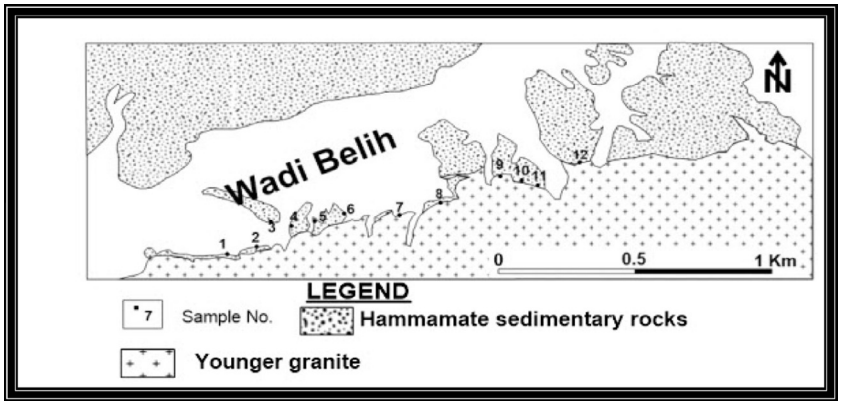

Figure 22 Location map for the collected samples of W. Belih area.

Table 2 Radiometric analyses of some samples collected from W. Belih area.

Rock type	Sample No.	eU (ppm)	eTh (ppm)	*K* (%)	eU/eTh
Hammamat sediments	1	4	4.5	1.5	0.9
	2	6.5	19	4	0.34
	3	9	15	5	0.6
	4	6	20	3	0.3
	5	11	33	2.3	0.33
	6	8	14.1	5.3	0.06
		Av = 7.42	Av = 17.6	Av = 3.5	Av = 0.42
Mineralized Hammamat sediments	7	14,647	602	0.47	24.3
	8	700	40	5	17.5
	9	2900	200	4.6	14.5
	10	960	45	4.4	21.3
	11	1350	78	2	17.3
	12	800	30	3	26.7
		Av = 3559.5	Av = 165.8	Av = 3.2	Av = 20.3

Av = average.

NE–SW compression event and overprinted by oblique normal fault during the NW–SE extension regime which affected the W. Belih area. The gamma radioactivity measured along this fault gives over scale with an eU content of 14,647 ppm. The host rocks show intense sodic metasomatism represented by albite (Plate I), hematite alteration and the uranium mineralizations are closely associated with the rock alterations.

The X-ray diffraction for this anomaly indicated the presence of uranophane as secondary uranium minerals in association with albite (Na-metasomatism) (Plate I). These facts indicated that uranium mineralizations along W. Belih are associated with Na-metasomatism, this support the classification of W. Belih uranium mineralizations in the Hammamat sedimentary rocks as metasomatite uranium (U) deposit type. This coincides with [13] who studied the petrological and geochemical studies on the younger granites and the Hammamat sediments at W. Belih area and mentioned that; some samples show Na-metasomatism (albitization) alteration in altered granites and exhibit high uranium content.

The most important structural factor controlling these mineralizations is the NE–SW to ENE–WSW fault zone along which the hydrothermal fluids that carried the load of mineralizations were extruded and trapped. The deposition of uranium minerals is due to mixing of U-bearing fluids with meteoric water and fluid-wall rock interaction resulted in changes in pH and oxygen activity leading to deposition of U-minerals [14,23].

The second anomaly is founded as a lenticular zone of 10×1 m in dimensions (sample 9, Fig. 22). It is recorded in the altered siltstone staining the surfaces of tension joints parallel to normal fault striking from N50°E to N57°E (Fig. 24). The gamma radioactivity measured over this anomaly reaches to 8500 cps with eU content 2900 ppm. This anomaly also contains visible secondary uranium minerals. The NE–SW fault zone with its associated tension joints is the structural control of this radioactive and mineralized zone.

The ESEM study revealed the presence of secondary uranium mineral uranophane ($Ca(UO_2)\ 2Si_2O_7{\cdot}6H_2O$) in this anomaly (Plate II). Ref. [13] studied the mineralogy of

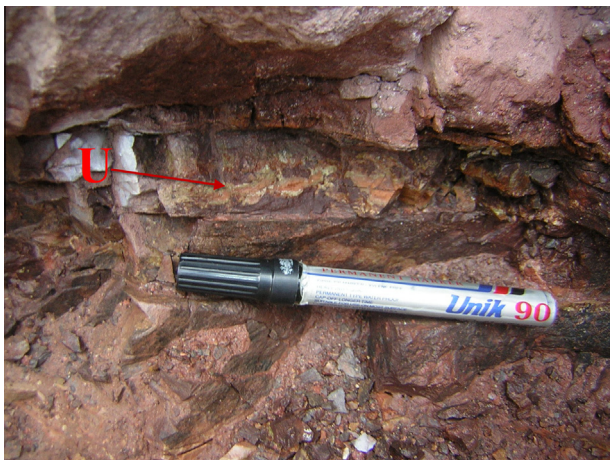

Figure 24 Radioactive uranium filling joints in bleached Hammamat with visible secondary uranium minerals, W. Belih area, looking S.

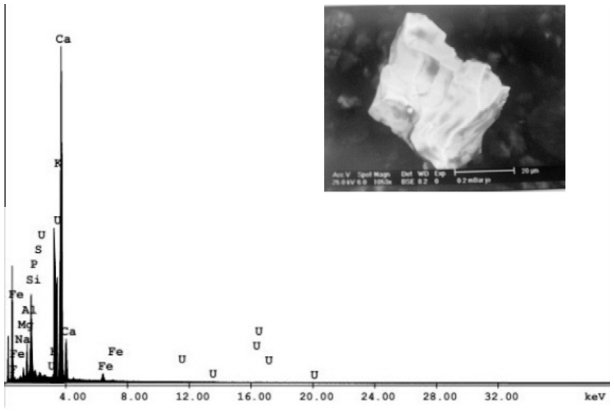

Plate II Back-scattered electron image and EDAX chart of uranophane ($Ca(UO_2)\ 2Si_2O_7{\cdot}6H_2O$).

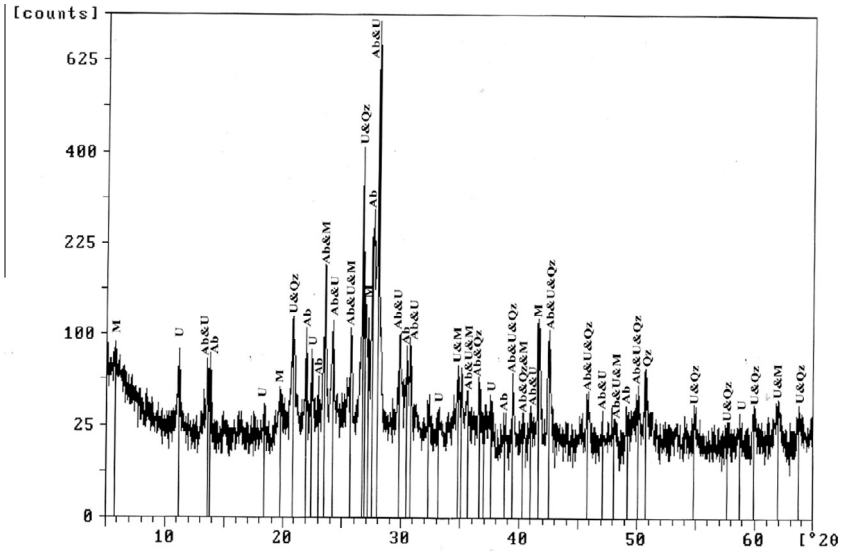

Plate I XRD detected the presence of uranophane (U) associated with albite (Ab), quartz (Qz) and montmorillonite (M).

mineralized zone of Hammamat sediments at W. Belih area, using X-ray diffraction and indicated the presence of uranophane as secondary uranium minerals.

The uraniferous Hammamat rocks located at the northern contact with Gabal (G.) Gattar granites were studied by [12]. They concluded that the secondary uranium mineralizations are mainly presented in the altered siltstones occupying joint surfaces and minute fractures.

There are other two radioactive anomalies located parallel to the contact between the Hammamat and younger granites (samples 10 and 11, Fig. 22) along joint sets trending N40°E with dips of about 43° to SE and N65°E with dipping of about 80° to SE. The gamma radioactivity measured at these anomalies reaches to 4000 cps and 5400 cps with eU content of 960 ppm and 1350 ppm respectively.

These steeply dipping tension joints striking from N40°E to N65°E due to the younger tension regime from NW–SE direction are the structural control for these two radioactive anomalies.

The phenomenon of uranium mineral distribution, at W. Belih area, is the localization of secondary uranium minerals along NE–SW to ENE–WSW fault zone and its associated joints along the contact between Hammamat and granites. The host rocks show intense sodic and hematite alteration and the uranium mineralizations are closely associated with these alterations (metasomatite uranium (U) deposit type).

4.1. Tectonic structures controlling U deposits

Uranium mineralizations are irregularly distributed in most metasomatic zones along the contact between the Hammamat sedimentary rocks and younger granites in the studied area, but the highest concentration occurs in the most intensively structurally deformed zones.

Metasomatite uranium mineralizations are located within the southern eastern limb of the W. Belih anticline along a fault zone (shear zone) in the Hammamat sedimentary rocks and episyenite, adjacent to the Gattarian granites. The mineralization is strongly linked to the fault activities. These faults strike NE–SW to ENE–WSW conformably with the bedding of the Hammamat and the northern granites injections. The major mineralization-controlling structures record a complex history of ductile and brittle deformation. The deposits are located along a fault which strikes ENE–WSW to NE–SW and dips 73° to SE (Fig. 23). The uranium mineralizations are located in the footwall. That fault was reactivated during its tectonic history starting from compression thrust to tensional diagonal normal and sinistral fault event during the youngest NW–SE extension regime which affected W. Belih area. Other uranium mineralizations are located along tension joints associated with pure normal fault striking N50°E and dipping 85° to SW (Fig. 24).

The brittle deformation features of that shear zone include the following criteria: Pegmatite and basic dykes extruded across the footwall of the shear zone; they are sub-vertical, weakly deformed with mainly thin thickness and other is very thick (Figs. 25 and 26). It strikes NE–SW parallel to the contact.

The episyenitization process is a feature to brittle deformation and almost occurs near the margins of the granitic pluton, closely associated with tectonic tensional deformations and fracturing. Several studies of the episyenitized granites show that, they occur as irregular bodies related to major faults and tension fracture zones [24–26]. In addition to, fractures and steeply dipping tension joints striking from N25°E to N75°E reflecting younger tension regime from NW–SE direction.

Figure 25 Pegmatite dyke extruded across the footwall of the shear zone, W. Belih area, looking NE.

Figure 26 Sub-vertical basic dyke striking along the north east direction parallel to the contact, W. Belih area, looking SW.

Due to the resulting tension, the hydrothermal solution gradually migrates upward where K and Na-metasomatite are developed along the faults and associated with uranium. Na-metasomatic bodies comprise albitites passing outward to dequartzified granites (episyenite) and then to unaltered host rocks (Fig. 7). In addition, it is recognized that low-stress regions are the favorable locations for fluid focusing, implying that low-stress regions in the vicinity of a fault are favorable locations for fluid flow focusing and hence U mineralizations occur in the highly fractured and mylonitized zones along the contact as lensoidal bodies. This mechanism had been proposed to explain hydrothermal circulation driven by the intrusion of granites (Fig. 27).

It is clear that, there is a great relationship between structure activity and uranium mineralizations in the investigated area.

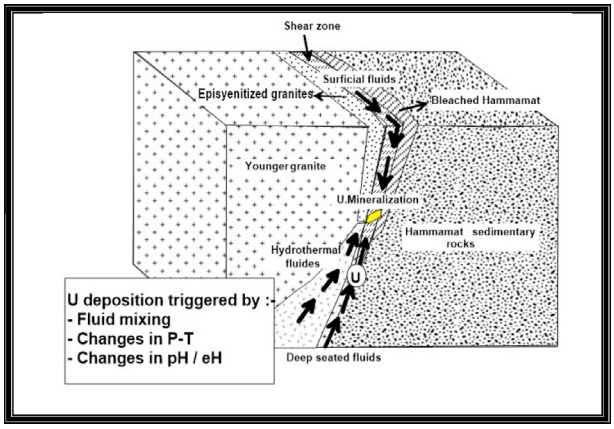

Figure 27 Schematic representation of essential ingredients in the formation of metasomatic uranium system along the structural contact between Hammamat sedimentary rocks and younger granite, W. Belih area.

5. Conclusion

Uranium mineralizations are irregularly distributed in most metasomatic zones along the structural contact between the Hammamat sedimentary rocks and the younger granites. X-ray diffraction indicated the presence of uranophane mineral in association with albite (Na-metasomatism) so that, uranium mineralizations of W. Belih are classified as metasomatite uranium (U) deposit type. But the highest concentrations are located in the most intensive structurally deformed zones. So, we can mention that the mineralizations are strongly linked to the fault activities. These faults strike NE–SW to ENE–WSW conformably with the bedding of the Hammamat sedimentary rocks. These faults providing a focused pathway for fluid migration with mineralizations concentrated along and adjacent to faults related to the tensional regime from NW–SE direction which affected W. Belih area.

The major uranium mineralizations controlling structures or shear zone record a complex history of compression and tension during its tectonic history, where the NW–SE compression event is the oldest compression event which affected the shear zone and induced the ENE–WSW reverse fault. This fault is reactivated as sinistral strike slip fault by the NE–SW compression event which represents the second event in the chronology along the contact area and also by the youngest NW–SE extension event. In addition, the youngest NW–SE extension event reactivates the NE–SW normal faults which is induced due to the post Hammamat sedimentary rocks pre-younger granite intrusion. Along these reactivated NE–SW normal faults the hydrothermal fluids that carried the load of mineralizations were extruded and trapped adjacent and along the fault zone or shear zone.

Acknowledgement

We thank the great help of Prof. Joseph Samaan in carrying out the electron microscope scan analysis.

Appendix A

See Appendix 1.

Appendix 1 Results of paleostress tensors determination along the contact between the Hammamat sedimentary rocks and the younger Gattarian granites, W. Belih area, Northern Eastern Desert, Egypt.

Site	Method	$\sigma 1$		$\sigma 3$		Φ	Type	Fault slip data diagram
		D	P	D	P			
1	P/T	215	29	125	3	0.5	CP	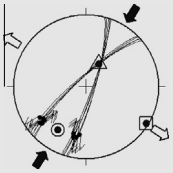
2	P/T	232	33	129	19	0.5	CP	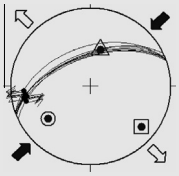
2	P/T	129	21	40	1	0.5	CP	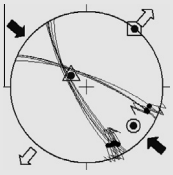

Appendix 1 (*continued*)

Site	Method	$\sigma 1$		$\sigma 3$		Φ	Type	Fault slip data diagram
		D	P	D	P			
3	P/T	230	30	139	3	0.36	CP	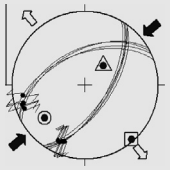
4	P/T	312	22	44	2	0.5	CP	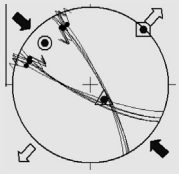
4	P/T	49	14	140	3	0.48	CP	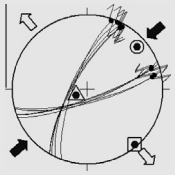
5	P/T	234	64	137	3	0.39	EXT	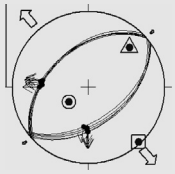
6	P/T	325	24	227	15	0.8	CP	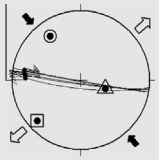
7	P/T	227	30	135	4	0.46	CP	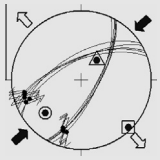
7	P/T	126	11	217	1	0.5	CP	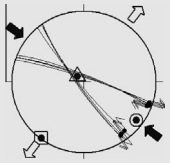
8	P/T	37	48	130	2	0.33	EXT	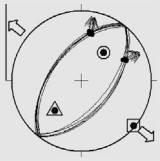
9	P/T	127	8	28	51	0.5	CP	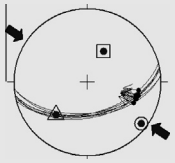
9	P/T	220	38	313	3	0.5	CP	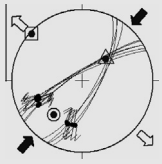

(*continued on next page*)

Appendix 1 (*continued*)

Site	Method	$\sigma 1$		$\sigma 3$		Φ	Type	Fault slip data diagram
		D	P	D	P			
12	P/T	234	58	143	1	0.5	EXT	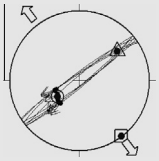
14	P/T	36	37	306	1	0.4	EXT	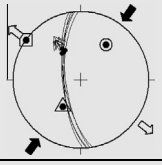

D, direction of plunge; P, amount of plunge; CP, compression; EXT, extension; P/T, pressure/tension axes method.

References

[1] M. Cuney, Miner. Deposita 44 (2009) 3–9.
[2] F.J. Dahlkamp, Uranium Deposits of the World, Springer, Berlin Heidelberg, New York, 2009, p. 2400.
[3] O.P. Kreuzer, V. Markwitz, A.K. Porwal, T.C. McCuaig, Ore Geol. Rev. 38 (2012) 334–366.
[4] M.I. Pownceby, C. Johnson, Ore Geol. Rev. 56 (2014) 25–44.
[5] M. Cuney, A. Emetz, J. Mercadier, V. Mykchaylov, V. Shunko, A. Yuslenko, Ore Geol. Rev. 44 (2012) 82–106.
[6] A.B. Salman, M.H. Shalaby, L.M. Noseir, Int. Earth Sci. Congr. Reg. 1 (1994) 89–101.
[7] M.E. Roz, Geology and uranium mineralizations of Gabal Gattar area, North Eastern Desert, Egypt (M.Sc. thesis), Fac. Sci., Al Azhar Univ., Egypt, 1994, p. 175.
[8] M. Abu Zaid, Relation between surface and subsurface uranium mineralizations and structural features, Gabal Gattar, North Eastern Desert, Egypt (M.Sc. thesis), Fac., Sci., Ain Shams Univ., 1995, p. 208.
[9] M.C. Haridy, Physical and mechanical properties of Gabal Gattar Granitic Pluton and the relation to joint-type U-mineralizations (M.Sc. thesis), Faculty of Science, Cairo Univ., 1995, p. 170.
[10] E.M. Esmail, Subsurface geological study of Wadi Beli uranium occurrence, North Eastern Desert, Egypt (M.Sc. thesis), El Azhar Univ., 2002, p. 204.
[11] M.H. Shalaby, 7th Conf. Phanerozoic and Develop, 3, Al Azhar Univ., Cairo, 1990, p. 19.
[12] M.A. Mahdy, A.B. Salman, A.H. Mahmoud, 14th Congress of Mining and Metallurgy, Edinburgh, Scotland, 1990, pp. 229–235.
[13] A.A. Mahdy, Petrological and geochemical studies on the younger granites and Hammamat sediments at Gabal Gattar-5 uranium occurrence, Wadi Balih, North Easter Desert, Egypt (Ph.D. thesis), Geology, Dept., Faculty of Science, Ain Shams Univ., 1999, p. 198.
[14] A.M. El-Kammar, A.E. Salman, M.H. Shalaby, A.I. Mahdy, Chem. J. 35 (2001) 117–135.
[15] M.H. Shalaby, A.F. Moharem, Sediment. Soc. Egypt 9 (2001) 145–155.
[16] N.F. Amin, Surface and subsurface structural features controlling uranium mineralizations at granitic-Hammamat contact, Wadi Belieh, Northern Eastern Desert, Egypt (Ph.D. thesis), Faculty of Science, Ain Shams University, 2010, p. 98.
[17] N.M. Mahdy, M.H. Shalaby, H.M. Helmy, A.F. Osman, E.H. El-Sawy, E.K. Abu Zeid, Arab J. Geosci. (2013), http://dx.doi.org/10.1007/s12517-013-0933-2.
[18] M. Cathelineau, J. Petrol. 27 (4) (2001) 944–965.
[19] A.A. Abdel-Hamid, Geologic factors controlling the radon emanation associated with uranium mineralizations along Wadi Belieh, North Eastern Desert, Egypt (M.Sc. thesis), Geology Dept., Faculty of Science, Benha Univ., 2006, p. 189.
[20] A. Etchecopar, Etude des états de contraintes en tectonique cassante et simulation de deformations plastiques (approche mathématique) (These Doctorat-es-Sciences), Univ. Sciences, et Techniques Languedoc, Montpellier, 1984, p. 270.
[21] F.J. Turner, Am. J. Sci. 251 (1953) 276–298.
[22] D. Delvaux, B. Sperner, Geol. Soc. London Spec. Publ. 212 (2003) 75–100.
[23] H.M. Helmy, R. Kaindl, T. Shibata, Ore Geol. Rev. (2014), http://dx.doi.org/10.1016/j.oregeorev.2014.03.008.
[24] U. Halenius, J.A.T. Smellie, Neues Jahrb. Mineral. Abh. 147 (1983) 229–252.
[25] L. Hecht, W. Spicgel, G. Morteani, in: H.W. Haslam, J.A. Plant (Eds.), Granites, Metallogeny, Lineaments and Rock-Fluid Interactions. Report SP/94/1, British Geol. Surv., Keyworth, Nottingham, 1994, pp. 220–243.
[26] J. Petersson, T. Eliasson, Lithos 42 (1997) 123–146.